Statics and Dynamics of Fluorescent Lamps Operating at High Frequency: Modeling and Simulation

Shmuel Ben-Yaakov, Moshe Shvartsas, and Stanislav Glozman

***Abstract*—The static and dynamic response of a fluorescent lamp operating at high frequency was studied and modeled by a SPICE-compatible behavioral equivalent circuit. Good agreement was found between model simulations and experimental results. It was also found analytically that the proposed model predicts a zero at the right half-side of the complex plane as observed experimentally.**

***Index Terms*—Electronic ballast, fluorescent lamp, SPICE models, SPICE simulation.**

I. Introduction

IT IS WELL documented that the electrical V–I characteristic of a fluorescent lamp under high-frequency (HF) excitation is, to a first approximation, resistive [1]. Indeed, for many practical purposes the lamp can be replaced by an equivalent linear resistor [2], [3]. However, a closer examination of fluorescent lamps characteristics reveals that this approximation is very crude and does not take into account many intricate phenomena that may be significant in the analysis and design of electronic ballasts. The deviations from the linear resistor model can be divided into three categories: the dependence of the V–I curve on the lamp's power level [4]–[6], the nonlinearity of the V–I curve at a given operating condition [7], [8], and the time-domain response of the lamp to a change in excitation [9], [10]. The latter aspect has many theoretical and practical implications since the dynamics of the lamp are of prime importance when considering stability and response of lamp/ballast systems in open- and closed-loop configurations [10]. Furthermore, the nature of the dynamic response must be seriously considered in applications that call for modulation of the lamp's "carrier" signal [11]. It is, thus, clear that a SPICE-compatible model that will emulate the electrical static and dynamic characteristics of fluorescent lamps operating at HF could be highly useful from the practical and theoretical points of view.

The objective of this study was to develop a SPICE-compatible model that will exhibit two major electrical features of the fluorescent lamp operated at HF: the dependence lamp's resistance on power level and its dynamic response to changes in electrical excitation. It is still assumed that, at any given operating point, the lamp is resistive. Based on experimental observations as well as some physics-based reasoning, we developed a behavioral model to emulate the electrical response of a fluorescent lamp. Once developed, the model was calibrated against experimental data and then verified by independent measurements.

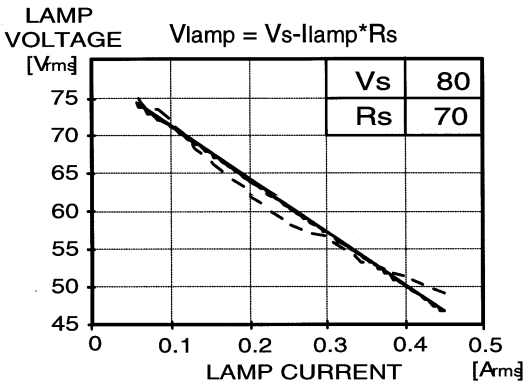

Fig. 1. Lamp voltage versus lamp current (OSRAM L 18 W/10). Broken line: experimental; solid line: linear fit.

II. Observations

As reported earlier, the impedance of fluorescent lamps operation at HF is approximately resistive. Following [4], the equivalent resistance $(R_{\rm eq})$ at HF can be expressed as

$$R_{\rm eq} = \frac{V_s}{I_{\rm rms}} - R_s \tag{1}$$

where V_s and R_s are the lamp's constants and $I_{\rm rms}$ is the rms current through the lamp.

Relationship (1) is valid for a limited power range from about 30% to nominal power. For a wider power range, the $V_{\rm lamp} = f(I_{\rm lamp})$ is nonlinear and, hence, a higher order polynomial is required to fit the lamp's characteristic. This issue is further discussed in Section VII. The parameters of (1) (V_s, R_s) can be obtained from experimental data [4]. The degree of matching is depicted in Fig. 1. The linear curve fitting for this lamp (OSRAM L 18 W/10) yields the constants: $V_s = 80$ V and $R_s = 70\ \Omega$.

The dependence (1) is for static conditions (constant HF drive). That is, at steady state conditions the HF V–I curve of

Paper MSDAD-A 02–26, presented at the 1999 IEEE Power Electronics Specialist Conference, Charleston, SC, June 27–July 1, and approved for publication in the IEEE TRANSACTIONS ON INDUSTRY APPLICATIONS by the Production and Application of Light Committee of the IEEE Industry Applications Society. Manuscript submitted for review June 24, 2000 and released for publication August 26, 2002. This work was supported by a grant from the Israel Science Foundation.

The authors are with the Power Electronics Laboratory, Department of Electrical and Computer Engineering, Ben-Gurion University of the Negev, Beer-Sheva 84105, Israel (e-mail: sby@bguee.ee.bgu.ac.il).

Digital Object Identifier 10.1109/TIA.2002.804745

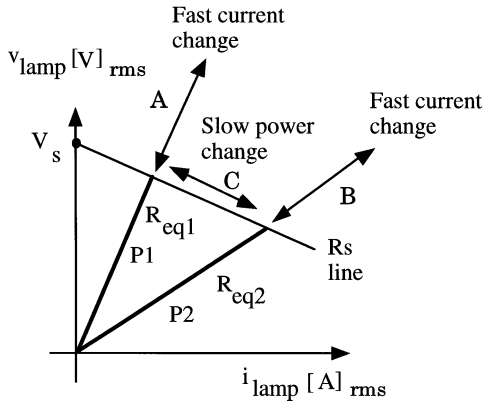

Fig. 2. Dynamic changes of V–I characteristics of a fluorescent lamp operating at HF.

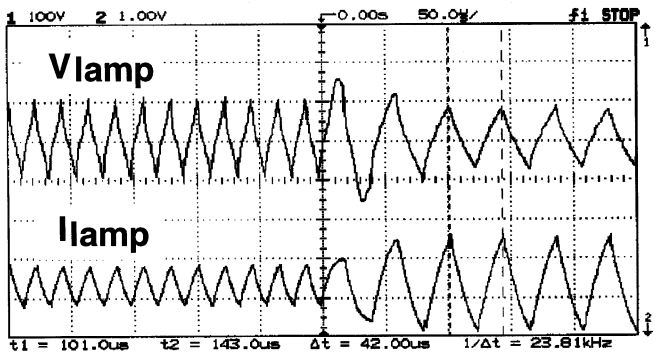

Fig. 3. Response of a fluorescent lamp voltage (upper trace, 100 V/div) and current (lower trace, 1 A/div) to a change in power level. Scale: 50 ms/div (horizontal). Lamp: OSRAM L 18 W/10. Carrier was stepped from 50 to 25 kHz.

the lamp depends on the power (or rms current) of the lamp as shown in Fig. 2. For a low power (P1), the lamp represents a relatively high resistance $(R_{\rm eq1})$, while at a higher power (P2), the resistance is smaller $(R_{\rm eq2})$. For a fast current change the response is approximately linear (arrows A and B, Fig. 2) while for a slow change in rms current the V–I curve will slide along arrow C (Fig. 2). The physical interpretation of this observation is linked to the lamps time constant associated with the generation/recombination of charge carriers in the lamp's plasma. A fast current change does not alter appreciably the density of the charge carriers in the plasma. Consequently, the lamp behaves (to a first approximation) as a linear resistor. For slow changes, the density of the carriers in the plasma will change and, hence, the resistance will shift. This behavior is clearly observed when exposing the lamp to a step change in the power level (Fig. 3). In this experiment, the lamp was driven by a square-wave voltage source in series with an inductor. The power level change was forced by changing the excitation frequency from 50 to 24 kHz. For the HF carrier, the lamp behaves as a linear resistor. The response to a change of power level (Fig. 3) is associated with a low-frequency time constant that controls the rate at which the resistance of the lamp is varying. It is postulated here that, for relatively small power variations, the response is associated with a single low-pass time constant (pole).

The dynamic response of the fluorescent lamp, discussed above, can be observed from a different angle: exposing the lamp to a modulated HF signal [9], [10]. In this case, the nature of incremental (modulation) resistance should be a function of the modulating frequency. This is depicted in the experimental results of Fig. 4. At low modulating frequency [Fig. 4(a)], the current and voltage variations are in the opposite direction, implying that the incremental resistance is negative. This can be explained by the fact that the V–I curves wobble along the path "C" of Fig. 2, which represents a negative resistance. For a high modulating frequency [Fig. 4(c)], the charge carrier density in the plasma is about constant and the incremental resistance is positive. In this case, the V–I trace is moving along the HF resistance (paths A and B, Fig. 2).

III. Model Development

Considering the above observations, it is evident that the electrical response of the lamp can be emulated by a behavioral dependent source whose resistance is defined by (1) [4], [5]. Equation (1) can be modified to a dynamic model if the rms current is first derived by measuring the lamp's rms current and then passing it through a low-pass filter that matches the slow response of the lamp. This slowly varying rms value can then be plugged back into (1) so as to change the lamp's resistance according to its static and dynamic behavior. The proposed SPICE-compatible model of Fig. 5 follows these ideas. In this model, the lamp is represented as a dependent current source (G_1) that emulates a variable resistance according to (1). The output of the dependent voltage source E_1 is proportional to the square of the lamp current $(i(\text{lamp}))$. Namely, the voltage at node (isq) is

$$v(\text{isq}) \equiv i[(\text{lamp})]^2 \tag{2}$$

where the notation $v(x)$ means the voltage at node "x." This $\{v(\text{isq})\}$ signal is then passed through a low-pass filter (R_1C_1, Fig. 5) to obtain its low-frequency component. For frequencies $f > 1/(2\pi R_1C_1)$ and for times $t > R_1C_1$, the average voltage on C_1 (node (p)) will be

$$v(p) = \frac{1}{T}\int_0^T v(\text{isq})dt \equiv \frac{1}{T}\int_0^T [i(\text{lamp})]^2\,dt \tag{3}$$

where T is the time constant R_1C_1.

The average voltage across the capacitor C_1 (node "p" in Fig. 5) is thus a smoothed value of the squared rms current. The filtered $I_{\rm rms}$ is then obtained by E_2 (node "rms" in Fig. 5) as the square root of the average voltage across the capacitor C_1 (node "p"). Consequently, the voltage at node rms, $v(\text{rms})$,

$$v(\text{rms}) \equiv \sqrt{\frac{1}{T}\int_0^T [i(\text{lamp})]^2\,dt}. \tag{4}$$

The definitions of the dependent sources are, thus, (per the notation of Fig. 5)

$$G_1 \equiv \frac{v(\text{lamp})}{\dfrac{V_s}{v(\text{rms})} - R_s} \tag{5}$$

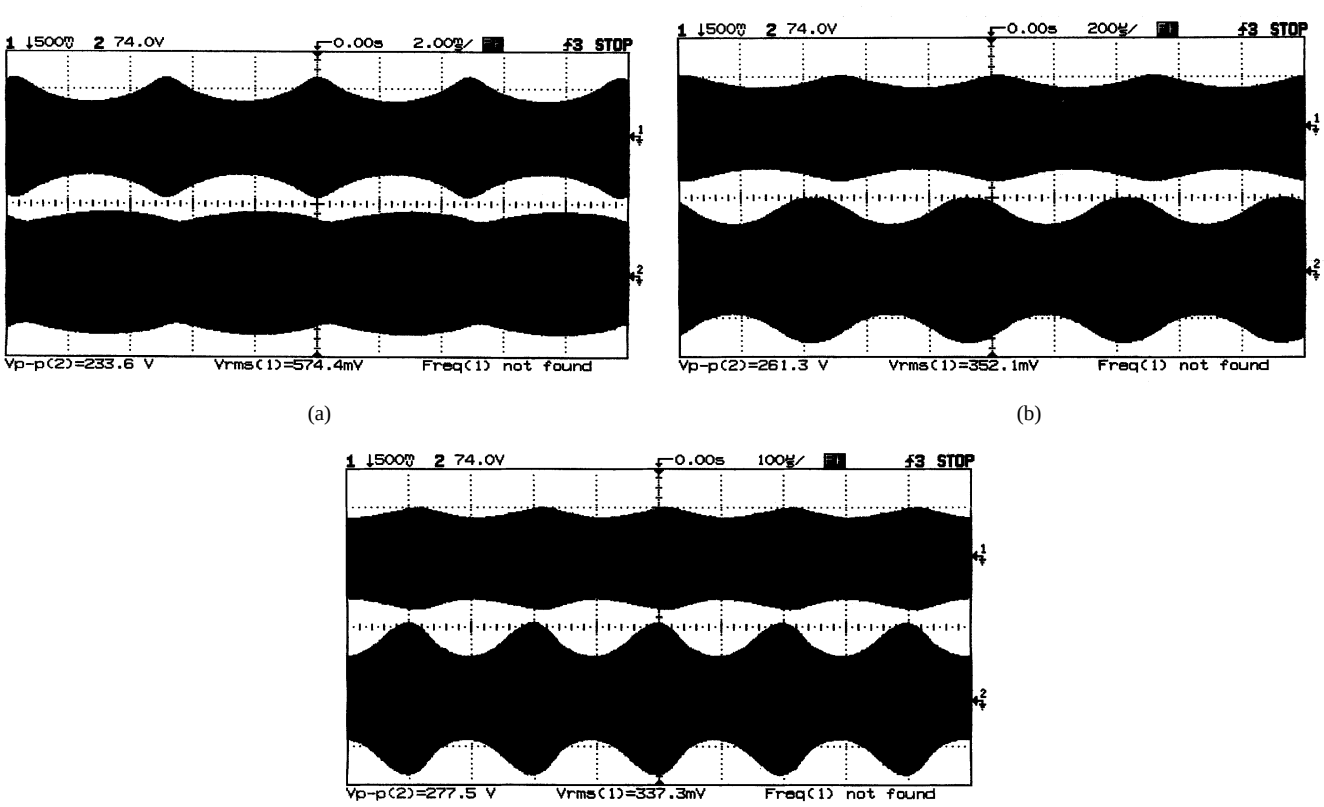

Fig. 4. Response of a fluorescent lamp (OSRAM L 18 W/10) to a modulation on the HF excitation. Modulation frequency: (a) 200 Hz, (b) 2 kHz, and (c) 5 kHz. Upper traces: lamp current (0.5 A/div); lower traces: lamp voltage (74 V/div); carrier frequency: 50 kHz.

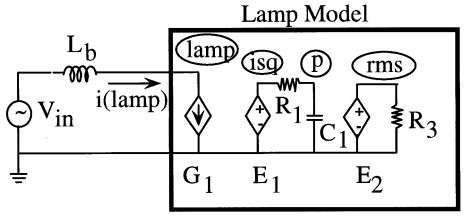

Fig. 5. Proposed fluorescent lamp model connected to HF ballast.

$$E_1 \equiv \{i(\text{lamp})\}^2 \tag{6}$$

$$E_2 \equiv \sqrt{v(p)}. \tag{7}$$

The dynamic response of this model to changes in power level clearly depends on the time constant R_1C_1. It is postulated and subsequently proven that this single time constant can produce the observed dynamic responses of the physical lamp.

IV. Small-Signal Response

The response of the proposed model (Fig. 5) to a modulated signal on the carrier can be derived from (1). The key parameter is the lamp's incremental impedance $(Z_{\text{inc}}(f_L))$, defined as the ratio of the modulating voltage component to the superimposed current. It is derived by first representing (1) in a way that will

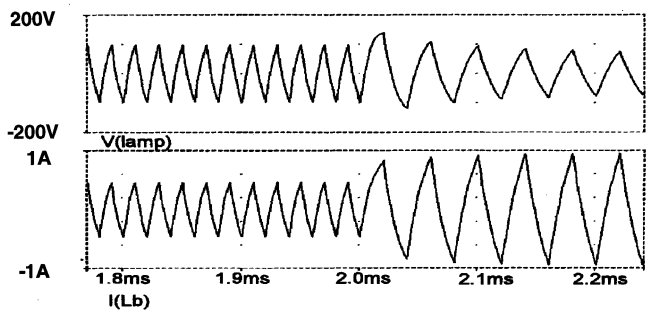

Fig. 6. Simulated response of a fluorescent lamp voltage (upper trace, 100 V/div) and current (lower trace, 1 A/div) to a change in power level. Simulation was carried out by the model of Fig. 5 for the experimental conditions of Fig. 3.

distinguish between the ac voltage and current of the lamp and the filtered component of the lamp's current

$$\tilde{V}_{\text{lamp}} = \tilde{I}_{\text{lamp}} \left(\frac{V_s}{I_{\text{lamp}_0}} - R_s \right) \tag{8}$$

where

$\tilde{V}_{\text{lamp}}$ lamp voltage (modulated phasor);
$\tilde{I}_{\text{lamp}}$ lamp current (modulated phasor);
I_{lamp_0} lamp rms current (time-dependent scalar).

The small-signal relationship is obtained by taking the derivative of (8)

$$v = i \left(\frac{V_s}{I_{\text{lamp}_0}} - R_s \right) - I_{\text{lamp}_0} \frac{V_s i_0}{\left(I_{\text{lamp}_0}\right)^2} \tag{9}$$

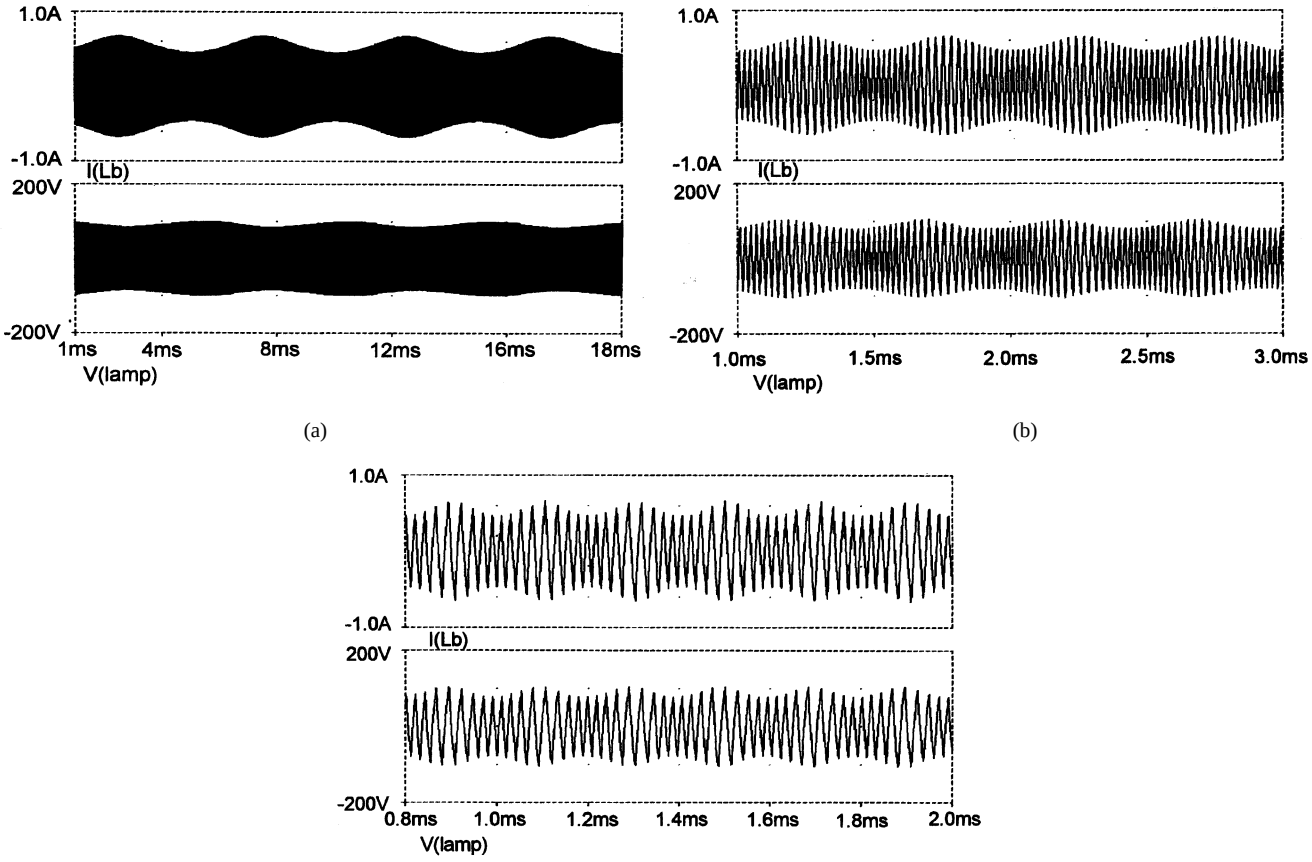

Fig. 7. Simulated response of a fluorescent lamp to a modulation on the HF excitation. Simulation was carried out by the model of Fig. 5 for the experimental conditions of Fig. 3.

where

v small-signal sinusoidal perturbation of $\tilde{V}_{\text{lamp}}$;
i small-signal sinusoidal perturbation of $\tilde{I}_{\text{lamp}}$;
i_o small-signal sinusoidal perturbation of I_{lamp_0}.

The small-signal component i_o is obtained by passing the lamp current through the transfer function $H(j\omega)$ of the low-pass filter (Fig. 5) as derived in the Appendix

$$i_0 = iH\left(j\omega\right). \tag{10}$$

From (9) and (10),

$$v = i\left(\frac{V_s}{I_{\text{lamp}_0}} - R_s\right) - \frac{V_s i}{I_{\text{lamp}_0}} H\left(j\omega\right) \tag{11}$$

or

$$v = i\left(\frac{V_s - R_s I_{\text{lamp}_0} - V_s H\left(j\omega\right)}{I_{\text{lamp}_0}}\right). \tag{12}$$

The transfer function of the low-pass filter is

$$H\left(j\omega\right) = \frac{1}{1 + j\omega T}$$

where $T = R_1 C_1$. From which

$$v = i\left(\frac{\left(V_s - R_s I_{\text{lamp}_0}\right)\left(1 + j\omega T\right) - V_s}{I_{\text{lamp}_0}\left(1 + j\omega T\right)}\right). \tag{13}$$

The lamp's incremental impedance (Z_{inc}) is, thus,

$$Z_{\text{inc}} = \frac{v}{i} = \left(\frac{\left(V_s - R_s I_{\text{lamp}_0}\right) j\omega T - R_s I_{\text{lamp}_0}}{I_{\text{lamp}_0}\left(1 + j\omega T\right)}\right) \tag{14}$$

or

$$Z_{\text{inc}} = R_s\left(\frac{\frac{R_{\text{eq}}}{R_s} j\omega T - 1}{j\omega T + 1}\right). \tag{15}$$

Hence, the response of the proposed lamp model (Fig. 5) when driven by high carrier frequency which is modulated by a low frequency (f_L) is found to be

$$Z_{\text{inc}}(f_L) = R_s \frac{\frac{jf_L}{f_0}\frac{R_{\text{eq}}}{R_s} - 1}{\frac{jf_L}{f_0} + 1} \tag{16}$$

where $f_o = 1/(2\pi R_1 C_1)$. It is of great interest to observe that the response of the proposed model (16) includes a pole and a zero at the right half-side of the complex plane (RHPZ) as discussed in [9] and [10]. The reactive nature of the function is a result of the fact that the lamp, and proposed model, include an internal feedback of a low-pass nature $\{f(\text{cutoff}) = 1/(2\pi R_1 C_1)\}$. The phase shifts associated with this feedback path make the incremental impedance look reactive.

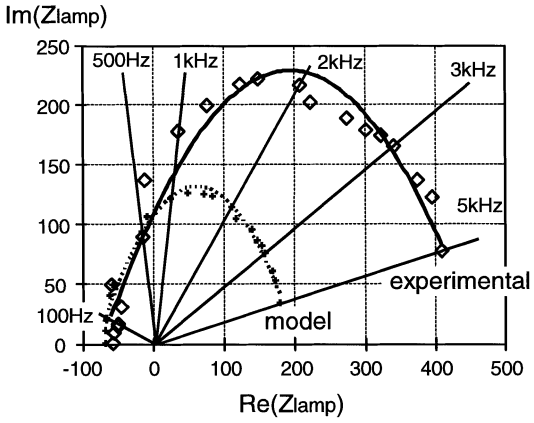

Fig. 8. Complex plan plot of measured and simulated incremental impedance of a fluorescent lamp (in ohms). Carrier frequency 50 kHz, modulation frequency as marked.

The mathematical representation of (16) is in excellent agreement with the physical reasoning given above in connection with Fig. 2. For low modulation frequency $(f_L \to 0) Z_{\rm inc}(f_L) \to -R_s$ and for high modulating frequency $(f_L \to \infty)\ Z_{\rm inc}(f_L) \to R_{\rm eq}$, as expected.

V. Model Calibration

The proposed model of Fig. 5 can be calibrated to the response of a given lamp by evaluating V_s, R_s, and the time constant R_1C_1. The first two can be obtained by measuring the rms voltage and current of the lamp for various power levels as shown in Fig. 1. R_1C_1 can be obtained by matching the incremental response of the model to experimental results similar to those of Fig. 4. This was done experimentally by driving the experimental lamp by an HF carrier that was phase modulation (PM) modulated. The PM modulation causes an amplitude modulation (AM) due to the series inductor of the ballast [9], [10]. The lamp current and voltage traces are then used to identify the location of the low-frequency pole ($T = R_1C_1$ of Fig. 5). Since only the time constant is of importance, one of the components (say, C_1) is chosen arbitrarily while the other is calculated from the experimentally measured T.

VI. Experimental Results

Experiments were conducted on an 18-W lamp (OSRAM L 18 W/10) for which the model parameters were extracted as discussed above. Calibration of the time constant yielded the values: $R_1C_1 = 0.1$ ms corresponding to a cutoff frequency of about 1.7 kHz. A similar value was found for other lamps, of different shapes and higher or lower wattage, but this was not surveyed in detail in this study. For this lamp, we found that $V_s = 80$ V and $R_s = 70\ \Omega$. The degree of matching for the experimental lamp is shown by repeating the step (Fig. 6) and modulated (Fig. 7) responses. These should be compared to Figs. 3 and 4, respectively. As can be seen, the behavioral matching is very good. A more rigorous comparison was made by examining a complex plan plot of the measured and simulated increment impedance (Fig. 8). This plot reveals that the model predicts faithfully the phase but has a considerable error

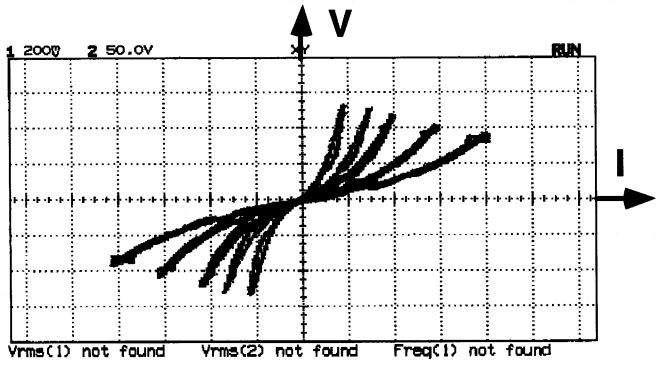

Fig. 9. V–I curves of experimental lamp when driven at 50 kHz for various power levels. Scales: 50 V/div (vertical); 200 mA/div (horizontal).

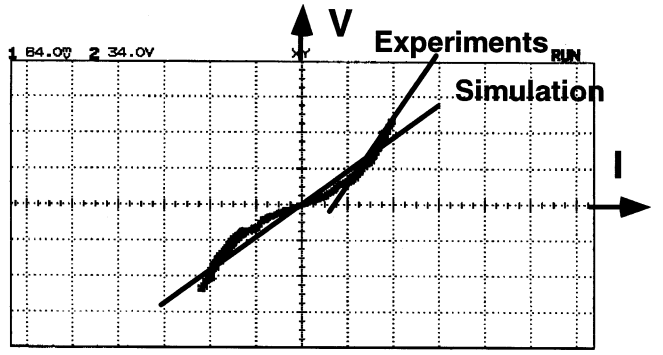

Fig. 10. Average equivalent resistance (Simulation) and peak equivalent resistance (Experimental). Scales: 34 V/div (vertical); 54 mA/div (horizontal).

in the amplitude. The reason for this discrepancy is traced down to the nonlinearity of the V–I curve of the experimental lamp (Fig. 9). The simulation model assumes a linear response at any power level (Fig. 10—Simulation). However, since the experimental measurements of the modulated component are made around peak values, they measure a higher incremental resistance (Fig. 10—Experimental).

VII. Discussion and Conclusions

The results of this study clearly suggest that the model of Fig. 5 is a good first-order approximation of fluorescent lamp behavior under static and dynamic conditions. The main reason for the deviation between the experimental and simulation results is the assumption that the lamp behaves as a linear resistor.

Implementation of the nonlinearly of the V–I curve (Figs. 9 and 10) [7], [8] may render an even more accurate model.

Implementation of this extra correction has not been attempted at this time, as it required extensive polynomial fitting over the entire operating range. However, the basic features of the present model are already very useful. It emulates the static and dynamic response of a fluorescent lamp operating at HF and exhibits the predicted zero at the right half-side of the complex plane (RHPZ) response [9], [10]. The model can, thus, be useful in simulating open- and closed-loop responses of lamp/ballast systems. When applying the model for a wide range of dimming, one has to take into account that (1) is valid over a small power range.

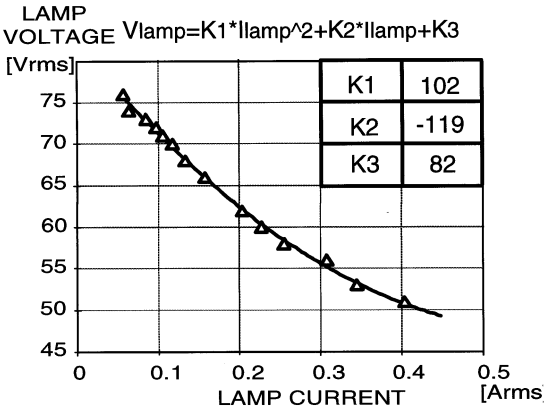

Fig. 11. Second-order polynomial fitting the lamp voltage versus lamp current. Same data as in Fig. 1.

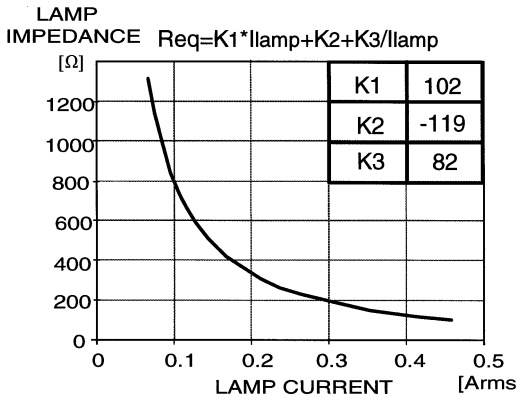

Fig. 12. Equivalent resistance of the experimental lamp derived from the data of Figs. 1 and 11.

If required, the fitting range can be extended by applying a second (or higher order) polynomial. For a second-order polynomial,

$$R_{\rm eq} = \frac{K_1}{I_{\rm rms}} + K_2 \cdot I_{\rm rms} + K_3 \tag{17}$$

where K_1–K_3 are constants of the lamp. This extension was found to emulate the behavior of the lamp over a 1:10 dimming range. For such a range, a second-order polynomial fitting seems a better choice (Fig. 11). Notice that, over this range, the lamp's equivalent resistance increases 15 fold (Fig. 12).

The proposed model (Fig. 5) can be used with any polynomial fitting. The only adjustment required is to replace the denominator of (5) by the expression of the equivalent resistance derived from the fitting by evaluating

$$\frac{V_{\rm lamp_{rms}}}{I_{\rm lamp_{rms}}} = f\left(I_{\rm lamp_{rms}}\right). \tag{18}$$

For the linear fit, the expression is that of (1). For a second-order polynomial, the expression is that of (17).

In the case of a high-order polynomial, the negative resistance R_s (1) varied with the operating point. It represents, in fact, the local slope of the $V_{\rm lamp_{(rms)}} = f(I_{\rm lamp_{(rms)}})$ curve. This local slope is derived automatically by the simulator when running the proposed model (Fig. 5).

Although developed through behavioral considerations, the model seems to suggest that the small-signal dynamics of the physical lamp is governed by a single time constant. The overall small-signal response is more complex, having both a pole and RHPZ due to the nonlinearly of (1) and the internal feedback to changes of power level. It is of interest to note that the time constant (R_1C_1) of 0.1 ms is typical of many fluorescent lamps probed (albeit not systematically) in this study. It stands to reason that this time constant is linked to a specific physical process within the lamp. This issue is left here as an open question for future studies.

Appendix
Derivation Details of (10)

We note that

$$(1+x)^2 \approx 1 + 2x \tag{19}$$

and

$$\sqrt{1+y} \approx 1 + \frac{y}{2} \tag{20}$$

where x and y are small numbers $(x, y \ll 1)$.

Assume now an rms lamp current $I_{\rm lamp_0}$ and a modulating rms signal

$$i = mI_{\rm lamp_0}, \qquad m < 1. \tag{21}$$

The time-domain signal will be

$$\sqrt{2}I_{\rm lamp_0}(\sin(\omega_c t)(1 + m\sin(\omega_m t)). \tag{22}$$

After passing the squarer ((6), E_1 in Fig. 5) the signal becomes

$$2I^2_{\rm lamp_0}(\sin(\omega_c t))^2(1 + 2m\,\sin(\omega_m t)) \tag{23}$$

where ω_c and ω_m are the carrier and modulating frequencies.

The signal will, thus, include the following components:

$$\frac{2I^2_{\rm lamp_0}}{2}(1 + 2m\sin(\omega_m t)) + I_{HF} \tag{24}$$

where I_{HF} are the harmonics of the carrier. The *RC* section (Fig. 5) will filter out these components.

Upon passing through the *RC* ($H(\omega)$ transfer function), the signal becomes (in time-domain notation)

$$I^2_{\rm lamp_0}(1 + 2m\sin(\omega_m t + \varphi))\,|H(j\omega)|\,. \tag{25}$$

That is, a dc component modulated by a low-frequency signal and modified amplitude ($|H(\omega)|$) and phase (φ) by $H(\omega)$.

After this signal passes through the square-root operation ((7), E_2 in Fig. 5), we obtain

$$I_{\rm lamp_0}(1 + m\sin(\omega_m t + \varphi))\,|H(j\omega)|\,. \tag{26}$$

The low-frequency component i_0 (in frequency-domain notations) is, thus, [(10) in the paper]

$$i_0 = I_{\rm lamp_0} mH(\omega_m) = iH(j\omega). \tag{27}$$

REFERENCES

[1] W. Elenbaas, Ed., *Fluorescent Lamps*. London, U.K.: Macmillan, 1971.

[2] M. C. Cosby Jr and R. M. Nelms, "A resonant inverter for electronic ballast application," *IEEE Trans. Ind. Electron.*, vol. 41, pp. 418–425, Aug. 1994.

[3] J. A. Donahue and M. M. Jovanovic, "The LCC inverter as a cold cathode fluorescent lamp driver," in *Proc. IEEE APEC'94*, 1994, pp. 427–433.

[4] M. Gulko and S. Ben-Yaakov, "Current-sourcing parallel-resonant inverter (CS-PPRI): Theory and application as a fluorescent lamp driver," in *Proc. IEEE APEC'93*, 1993, pp. 411–417.

[5] T.-F. Wu, J.-C. Hung, and T.-H. Yu, "A PSPICE circuit model for low pressure gaseous discharge lamps operating at high frequency," *IEEE Trans. Ind. Electron.*, vol. 44, pp. 428–431, June 1997.

[6] S. Ben-Yaakov, "Modeling the high frequency behavior of a fluorescent lamp: A comment on "A PSPICE circuit model for low pressure gaseous discharge lamps operating at high frequency" by T.-F. Wu, J.-C. Hung and T.-H. Yu [1]," *IEEE Trans. Ind. Electron.*, vol. 45, pp. 947–950, Dec. 1998.

[7] B. Hesterman and N. Sun, "PSPICE high frequency dynamic fluorescent lamp model," in *Proc. IEEE APEC'96*, 1996, pp. 641–647.

[8] T. Liu, K. J. Tseng, and D. M. Vilathgamuva, "A PSPICE model for the electrical characteristic of fluorescent lamps," in *Proc. IEEE PESC'98*, 1998, pp. 1749–1754.

[9] E. Deng, "I. Negative Incremental Impedance of Fluorescent Lamp," Ph.D. dissertation, California Institute of Technology, Pasadena, 1995.

[10] E. Deng and S. Cuk, "Negative incremental impedance and stability of fluorescent lamp," in *Proc. IEEE APEC'97*, 1997, pp. 1050–1056.

[11] D. K. Jackson, T. K. Buffaloe, and S. B. Leeb, "Fiat lux: A fluorescent lamp digital transceiver," *IEEE Trans. Ind. Applicat.*, vol. 34, pp. 625–630, May/June 1998.

Shmuel (Sam) Ben-Yaakov (M'87) was born in Tel Aviv, Israel, in 1939. He received the B.Sc. degree in electrical engineering from the Technion, Haifa, Israel, in 1961, and the M.S. and Ph.D. degrees in engineering from the University of California, Los Angeles, in 1967 and 1970, respectively.

He is presently a Professor in the Department of Electrical and Computer Engineering, Ben-Gurion University of the Negev, Beer-Sheva, Israel, where he also heads the Power Electronics Group. He served as the Chairman of the department during the period 1985–1989. His current research interests include power electronics, circuits and systems, electronic instrumentation, and engineering education. He also serves as a Consultant to commercial companies on various subjects, including analog circuit design, modeling and simulation, PWM and resonant converters and inverters, soft-switching techniques, and electronic ballasts for discharge lamps.

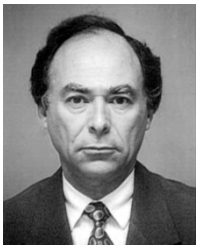

Moshe Shvartsas was born in Vilnius, Soviet Lithuania, in 1946. He received the Physicist Diploma from Vilnius State University, Vilnius, Soviet Lithuania, in 1967, and the Candidate of Technical Science (Ph.D.) degree from the St. Petersburg Institute of Labor Protection, St. Petersburg, Russia.

During 1967–1993, he was a Researcher with the R&D Institute of Electrical Welding Equipment, Vilnius. He specialized in welding generators, motor–generators, and noise reduction in welding electrical arcs. Since 1996, he has been a Co-Worker in the Department of Electrical and Computer Engineering, Ben-Gurion University of the Negev, Beer-Sheva, Israel. His current interests include electrical arcs, power supplies, and SPICE modeling.

Stanislav (Stas) Glozman was born in Tashkent, Uzbekistan, in 1972. He received the B.Sc. degree in electrical engineering in 1997 from Ben-Gurion University of the Negev, Beer-Sheva, Israel, where he is currently working toward the M.S. degree in electrical and computer engineering.

He is currently involved in a research program in the Power Electronics Group at Ben-Gurion University of the Negev. His fields of interest include fluorescent lamp modeling and electronic ballast design.